RSC Advances

PAPER

View Article Online
View Journal | View Issue

Cite this: *RSC Adv.*, 2020, **10**, 7259

Heavy metal adsorption using structurally preorganized adsorbent

Shuai Liang,[a] Shengguang Cao,[a] Changrong Liu,[a] Shah Zeb,[a] Yu Cui[a] and Guoxin Sun *[ab]

Heavy metal pollution is an essential environmental issue in the world. The current methods present limitations for the removal of low concentration divalent heavy metals from wastewater, such as high cost, unsatisfactory adsorption capacity, and poor reusability. Herein, we designed and prepared a novel chelating adsorbent. The adsorbent was prepared using chloromethyl polystyrene microsphere as a framework material modified by ethylenediaminetetraacetic acid (EDTA) with two types of functional groups and six binding sites in one coordination unit. Each coordination unit of the adsorbent prepared provides two negative charges of two carboxyl groups to balance the two positive charges of the divalent heavy metal ion, and forms coordination bonds through its two nitrogen atoms and two amidic carbonyl groups. This synergistic adsorption effect produced by electrostatic interaction and chelation significantly improves the adsorption capacity. The adsorption of some environmental heavy metals was tested, and high adsorption capacity for Pb(II) was obtained. The saturated adsorption capacity for Pb(II) was as high as 352.1 mg g^{-1}, and the effluent concentration of the column experiment was less than 0.20 ppm. Simultaneously, the presence of the amide group shows good anti-interference to alkali metals and alkali soil metals. The result is of considerable significance to the actual wastewater treatment.

Received 6th January 2020
Accepted 10th February 2020

DOI: 10.1039/d0ra00125b

rsc.li/rsc-advances

1 Introduction

Lead is a very toxic heavy metal widely applied in various industries. Over the past years, lead contamination has caused a wide range of environmental concerns.[1] The heavy metals in the environment could be transmitted along the food chain and accumulate in the body resulting in health problems.[2] The separation of lead from sewage has been an extensive concern for years. The removal methods of heavy metals from wastewater mainly include chemical precipitation, solvent extraction and solid adsorption.[3–6] Among them, solid adsorption has specific characteristics of simple operation and easy separation. Joseph carried out the adsorption of Pb(II) using kaolinite and smectite, and the relative adsorption capacities were MY22s 3.36 mg g^{-1} and Sa01 4.73 mg g^{-1}, respectively.[7] Anitha[8] reported that the maximum adsorption capacity of chitosan/PAN for Pb(II) was 20.08 mg g^{-1}. Ravishankar[9] prepared graphene oxide to test the adsorption of lead. Graphene oxide-based magnetic nano-sorbent was synthesized, and the adsorption capacity of the prepared nano-sorbent was estimated to be 73.52 mg g^{-1} with maximum removal of 93.78% at pH 6. It shows that it is challenging to obtain adsorbents with strong adsorption ability by simple functional groups, and the maximum adsorption capacity is not satisfactory.

Ethylenediamine tetraacetic acid (EDTA) is one of the widely used compounds with multiple sites to chelate with most of the metal ions powerfully. EDTA was modified on the surface of different materials to obtain strong adsorption of heavy metal ions. Jilal *et al.*[10] prepared cellulose derivatives based on EDTA and hydroxyethyl cellulose (HEC) and the Q_m values for Pb(II) and Cu(II) were 108.97 and 76.01 mg g^{-1}, respectively. EDTA modified multi-functionality of graphene oxide nanomaterials also gave high adsorption of Pb(II) and Cd(II) heavy metal ions.[11] Further studies showed that the alkali metals had little effect on the adsorption of heavy metals, but the competitive adsorption of alkali earth metal ions would significantly reduce the adsorption performance. Dan Lv[12] prepared a new bamboo activated carbon (BAC) with EDTA functionality and found that Mg^{2+} possessed the most considerable influence on the adsorption of Cu(II) because of a more substantial binding constant with EDTA. The EDTA-based layer exhibits higher adsorption efficiency owing to the stronger chelation of EDTA.[13] The distribution coefficient of Co(II) by EDTA–chitosan decreased significantly, which was most likely caused by the competitive binding of Ca(II).[14] Many water bodies polluted by heavy metal ions are rich in calcium and magnesium ions, so it is essential to develop adsorbents with a strong adsorption capacity of heavy metals and anti-interference against calcium and magnesium ions.

[a]*School of Chemistry and Chemical Engineering, University of Jinan, Jinan, 250022, Shandong, P. R. China. E-mail: sun-guo-xin@hotmail.com*
[b]*Institute for Smart Materials & Engineering, University of Jinan, Jinan, 250022, Shandong, P. R. China*

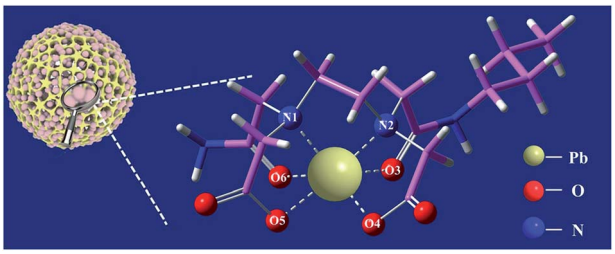

Fig. 1 The structure of EDBAMPS-metal chelate.

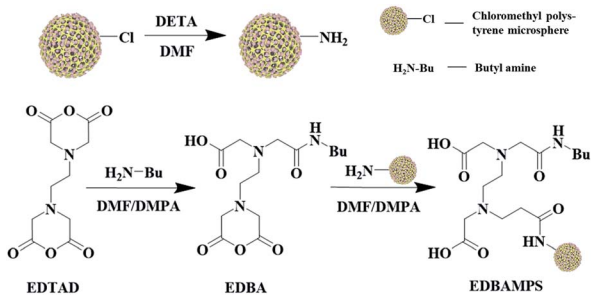

Fig. 2 Synthetic procedure of EDBAMPS.

To develop an adsorbent with strong adsorption capacity and good selectivity, we first analyzed the structure of heavy metal ions. The typical heavy metal ions, such as Pb(II) and Cu(II), usually formed a hexatactic architectural complex. Learning from the synergistic extraction principles, we designed new coordination units composed of two negative charges groups and four chelating groups. This structure satisfies the requirements of charge balance and six coordination (Fig. 1).

The novel chelating adsorbent contains two carboxyl groups (O4, O5) that correspond to the heavy metal valence state. Besides, the carbonyl group of two amides (O3, O6) and two amino nitrogen atoms (N1, N2) are involved in the formation of chelating coordination, which is beneficial to the coordination of multi orbital heavy metal ions. The binding ability of the adsorbent to calcium and magnesium and other small ions is reduced due to the modification of carboxyl groups by amide groups. So it is predicted that EDBAMPS should have excellent adsorption properties and selectivity.

2 Material and methods

2.1 Materials and synthesis

All the reagents used were analytically pure. Chloromethyl polystyrene microsphere was purchased from Tianjin Xingnan Yuneng Polymer Technology Co., Ltd. The diameter of microspheres is 200–600 μm, and the pore size between 5–6 nm, the specific surface area 44.81 $m^2\ g^{-1}$, and the pore volume $V_p = 0.31\ mL\ g^{-1}$.

2.2 Synthesis of EDBAMPS

The synthetic route of EDBAMPS was depicted in Fig. 2. Chloromethyl polystyrene microsphere (20.05 g) was treated with ethanol (100 mL) at rt for overnight. Then the solvent was removed by filtration. The obtained chloromethyl polystyrene microsphere was transferred into a 100 mL flask, then diethylenetriamine (30 mL) was added, and the mixture was stirred at 318 K for 12 h. After that, the excess diethylenetriamine was removed by ethanol washing, and an amino polystyrene microsphere was obtained (20.11 g).

Ethylenediamine tetraacetic anhydride (16.74 g, 65 mmol) and *n*-butylamine (4.75 g, 65 mmol) in *N*,*N*-dimethylformamide (DMF) (60 mL), and a catalytic amount of 4-dimethylaminopyridine (DMAP) were added into a 100 mL flask. The mixture was stirred at 338 K for 8 h, which afforded EDBA (10.75 g) as a brown powder.

4.12 g of amino microspheres, EDBA in 50 mL dry DMF, and catalyst DMAP were mixed at 65 °C for 24 h. After the reaction, the product was washed with anhydrous ethanol and distilled water. The canary yellow particles were vacuum dried overnight at 60 °C. Finally, the EDBAMPS (5.1 g) was obtained.

2.3 Adsorption procedure

0.10 g adsorbent and 5 mL 0.10 mmol L^{-1} heavy metal ion solution oscillated in a 10 mL stoppered test tube at a controlled temperature. 0.10 mmol L^{-1} different types of metal ions solution were employed. Metal ions concentration was measured by PinAAcle 900T USA atomic absorption spectrophotometer. X-ray photoelectron spectroscopy (XPS) was used to study the chelate structure formed on the surface of the adsorbent.

3 Results and discussion

3.1 Effect of pH

pH is one of the important factors affecting metal ions adsorption. The effect of pH-value on the adsorption process was presented in Fig. 3. At the lower pH value, H^+ in high concentration can compete with metal ions for the active sites to form protonation.[15] Therefore, the adsorption capacity decreased. With the increase of pH-value, the adsorption capacity of EDBAMPS towards metal ions was increased. The maximum adsorption capacity was obtained at pH 5.[16] As the pH value further rises to 5.5 or more, the existential form of Pb(II) in solution changes from Pb^{2+} to $Pb(OH)^+$, $Pb_4(OH)_4^{4+}$,

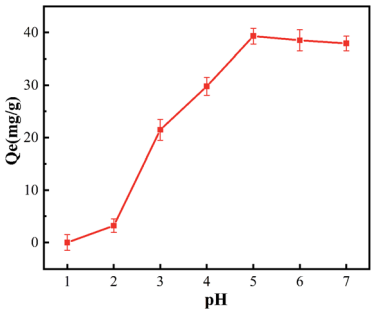

Fig. 3 Effect of pH-value on the adsorption capability of Pb(II) onto EDBAMPS.

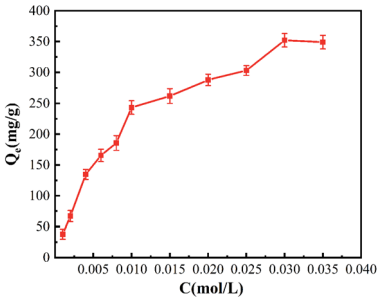

Fig. 4 Adsorption capacity of EDBAMPS towards Pb(II).

$Pb_3(OH)_4^{2+}$.[17] Due to steric hindrance and charge mismatch, the adsorbent coordination unit does not have strong adsorption ability to these species. This may be the reason why the adsorption amount shows a downward trend after a pH higher than 5.

3.2 Adsorption isotherms

The adsorption capacity of the resin with different concentrations of Pb(II) was shown in Fig. 4. And the adsorption isotherms for Pb(II) onto EDBAMPS was shown in Fig. 5. With the increase in initial metal concentration, the uptake of the metal ions was increased while the metal-removal efficiency decreased due to the earlier loading effect.[18]

The saturated adsorption capacity of Pb(II) was 352.1 mg g^{-1}. The adsorption data were fitted by Langmuir, Freundlich and Temkin models, and relevant parameters in Table 1. It revealed that the isotherm data could better be fitted by the Langmuir model. This shows that the uptake process was monolayer adsorption.[19] Each adsorption center only was dominated by an adsorbate molecule; it was no interaction between adsorbed molecules and formed immobile molecule layer.[20] According to the result of the Langmuir model calculation, the maximum metal adsorption capacity towards Pb(II) is 400 mg g^{-1}.

Table 2 gave some recently reported adsorbents. It can be seen that the adsorbent prepared by us has excellent adsorption performance, which should be attributed to the synergistic effect of functional groups at the adsorption site, which is consistent with our expectations.

3.3 Adsorption kinetics

Pb(II) adsorption behavior was investigated by using pseudo-first-order and pseudo-second-order models, and the fitting results are summarized in Fig. 6. It shows the influence of reaction time after the treatment of removal. It takes eight hours for the lead ions to reach adsorption equilibrium. The various kinetics parameters were calculated from the plots of kinetic model equations and are tabulated in Table 3. Obviously, the pseudo-second-order adsorption model was more suitable to describe the adsorption kinetics of Pb(II) onto the resin, and it relied on the assumption that adsorption might be the rate-limiting step.[32] The results illustrated that the chemical adsorption is the major of adsorption.[33]

3.4 Effect of common coexisting ions on the adsorption

K^+, Na^+, Ca^{2+}, and Mg^{2+} are common coexisting ions in the wastewater. Adsorbent resistance to interference from these ions is a practical requirement. In this part, we studied the effect of these ions on the adsorption of Pb(II). It is interesting that the adsorption efficiency of the adsorbent towards Pb(II) was enhanced with the increase in the concentration of Na^+, as shown in Fig. 7.

The adsorption efficiency of the adsorbent towards Pb(II) has also been evaluated in the solution containing other ions (K, Mg, Ca, 0.010 mol L^{-1}). The obtained result has been

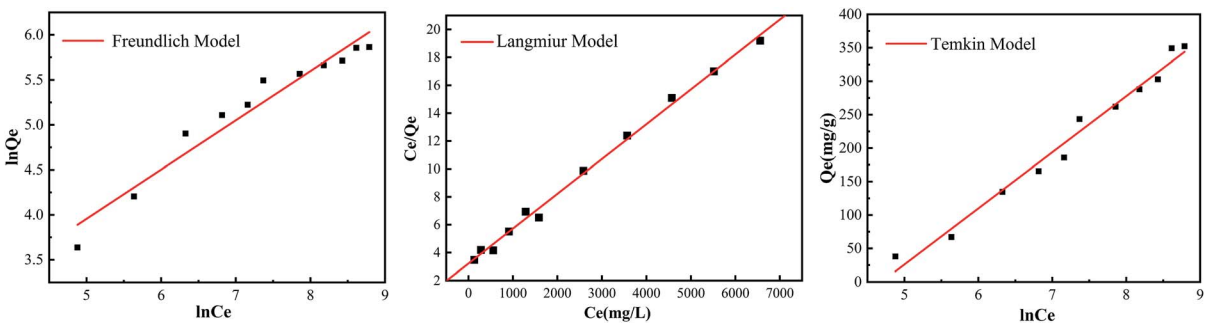

Fig. 5 Langmuir, Freundlich and Temkin models for Pb(II) onto EDBAMPS.

Table 1 Parameters of Langmuir, Freundlich and Temkin models for the description of Pb(II)

Langmuir			Freundlich			Temkin		
Q_m (mg g^{-1})	K_L (L mg^{-1})	R^2	K_F (mg g^{-1} (L $mg^{-1})^{1/n}$)	$1/n$	R^2	K_T (L g^{-1})	B	R^2
400	124.16	0.997	3.382	0.54751	0.974	0.0092	83.90	0.99

Table 2 Adsorption capability of Pb(II) with different adsorbents

Absorbents	Pb^{2+} (mg g^{-1})	Ref.
ZIF-8@GO	356	21
PBC@SiO_2–NH_2	120	22
Fe_3O_4@SiO_2@TCPP	798.34	23
g-C_3N_4/Mt	182.7	24
PEI@PDA/MS	231.8	25
(*N*-Cys)-functionalized bamboo lignin	58.8	26
ZIF-8@CA	1331.21	27
Spend mushroom compost biochar	564	28
PPy/TiO_2	237.03	29
GO/CNTS	98.1	30
SiNPz-Py	110.84	31
EDBAMPS	352.1	This work

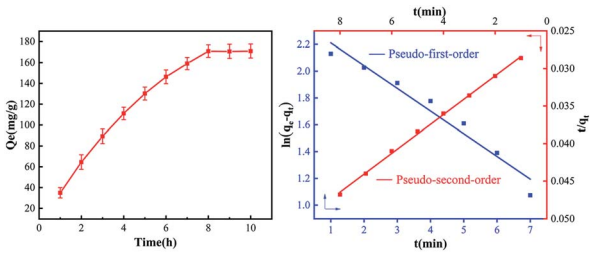

Fig. 6 The time for the lead ions to reach adsorption equilibrium; adsorption kinetics for Pb(II) onto EDBAMPS.

Table 3 Kinetics parameters for Pb(II) onto EDBAMPS

Pseudo-first-order		Pseudo-second-order	
k_1 (h^{-1})	R^2	k_2 (g mg^{-1} h^{-1})	R^2
0.39	0.978	0.0013	0.998

displayed in Table 4. The results indicated that the adsorption capability of adsorbent towards Pb(II) ions were much higher in the presence of divalent metal ions as compared with the monovalent metal ions. Instead of competitive adsorption, divalent alkaline earth metal ions promote the adsorption of

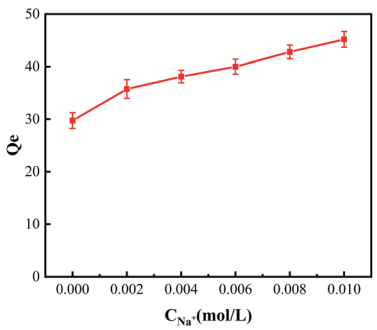

Fig. 7 Effect of competing ions on the adsorption capability of Pb(II) onto EDBAMPS.

Table 4 Adsorption amount for Pb(II) onto EDBAMPS under the presence of different metal ions

Metal ions	Blank	Na	K	Ca	Mg
Q_e (mg g^{-1})	30.00	45.17	43.62	53.46	60.19

heavy metals. This indicates that the modification of amides successfully reduces the chelating coordination with alkaline earth metal ions and prevents the competitive adsorption of these ions.

3.5 Adsorption of other metal ions

30 mg of resin and 5 mL of 0.10 mmol L^{-1} metal ions of different types of solution were placed in oscillating tubes and shaken in hydrothermal oscillator at 303 K for 8 h. Among them, the pH value of iron ions solution was kept 1 and 5 for Ni(II), Cu(II), Pb(II), Zn(II), Co(II), Ca(II) and Mg(II). The results of the adsorption of Ni(II), Cu(II), Pb(II), Zn(II), Co(II), Fe(III), Ca(II) and Mg(II) onto the adsorbent were presented in Fig. 8. It is clear from the data in Fig. 8 that when the concentration of ions was kept low in the solution, the removal rate of the Ni(II), Cu(II), Pb(II), Zn(II), Co(II) approached almost 100%. However, the removal rate for Fe(III) was slightly lower. In the case of alkaline earth metal ions, the adsorbent almost didn't show any adsorption capability for Ca(II) and Mg(II). This further illustrates that the introduction of amide groups enhances the selectivity of the adsorbent on metal ions. The adsorption capacity of alkaline earth metals was weakened. The concentration of residual after extraction was given in Table 5.

3.6 Recycling

The reuse of adsorbent is an important aspect of the actual application. Good repeatability reduces the use of materials used in the production process, hence saving costs. After the

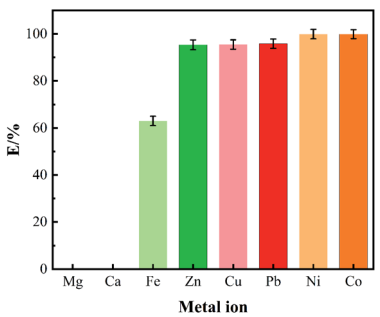

Fig. 8 Effect of competing ions on the adsorption capability of Pb(II) onto EDBAMPS.

Table 5 Residual ion concentration after extraction

Metal ions	Pb^{2+}	Ni^{2+}	Cu^{2+}	Co^{2+}	Zn^{2+}
Concentration (mg L^{-1})	0.85	0.059	0.29	0.059	0.31

adsorption of metal ions, the resins were desorbed by 1 mol L^{-1} of nitric acid for 4 h. Then vacuum drying the resin at 328 K in the thermostatic vacuum drier for 12 h. Dried resins were recycled in the adsorption process for 4 times. According to the experimental data given in Fig. 9, the activity of more than 90% adsorbent was still maintained after being used five times as adsorption & desorption cycles. These observations indicate that the adsorbent (EDBAMPS) was stable in reusability and hence could be used repeatedly for the removal of Pb(II) ions from wastewater.

3.7 Mechanisms

The Fourier Transform Infrared Spectrometry (FT-IR) was preferably done on selected batches of EDBAMPS, EDBAMPS-Pb is shown below in Fig. 10. The spectrum in this figure shows adsorption bands at various locations. The adsorption band at 1664–1641 cm^{-1} was ascribed due to the flexion of carbonyl in the amide group. The band at 1404–1388 cm^{-1} was due to the flexion of the C–O bond in the carboxylic group. The band at 1097–1091 cm^{-1} was assigned to the N–H bond in aliphatic amine. It could be observed that the spectra position of EDBAMPS-Pb had a red-shifted phenomenon. The result explained that these radicals were formed a coordination bond with metal ions, hence resulted in the displacement of spectral position.[34] These observed trends in FT-IR analysis revealed the adsorption mechanism of lead ions, which formed complexes with nitrogen and oxygen atoms in the polyamine resin.[35] But in this case, the mechanism could not explain the adsorption

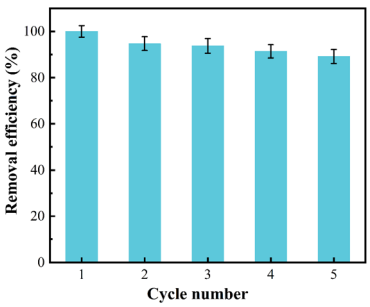

Fig. 9 Recycling adsorbent for adsorption capability of Pb(II) onto EDBAMPS.

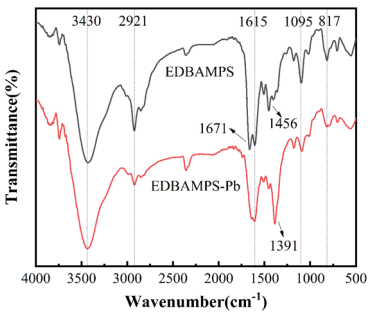

Fig. 10 FT-IR spectra of EDBAMPS before and after Pb(II) adsorption.

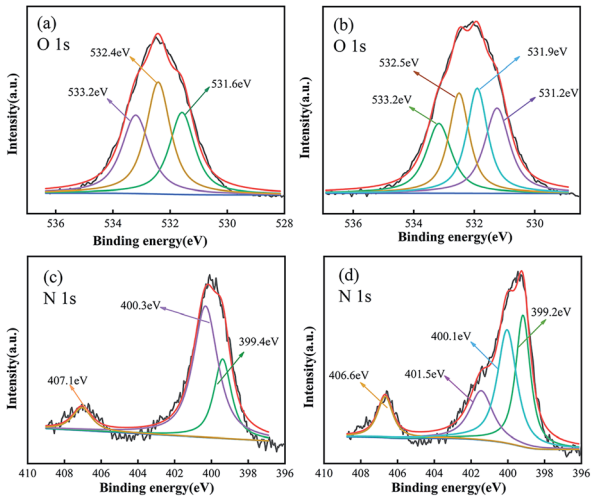

Fig. 11 High resolution O 1s spectra of (a) EDBAMPS and (b) EDBAMPS-Pb. High resolution N 1s (c) EDBAMPS and (d) EDBAMPS-Pb.

behavior effectively. It was due to the ability of metals forming the coordination bonds.[36]

In order to understand the nature of adsorption, the XPS spectra of blank adsorbent and heavy metal loading were collected, and the data were processed. The O 1s spectrum of the EDBAMPS in Fig. 11a can be fitted by three peaks around 533.2, 531.6, and 532.4 eV assigned to O 1s in C–O–H, –COOH, and C=O of amide groups, respectively.[21] The hydroxyl group may have been produced during the amination of the chloromethyl polystyrene microsphere. The surface hydroxyl group facilitates hydrophilicity and thus speeds up the adsorption process. After adsorption of lead ions, four peaks at 533.2, 532.5, 531.9, and 531.2 eV were found. This new peak at 531.9 eV should be attributed to the carboxyl binding of lead ions resulting in the difference between the two oxygen atoms. The peak at 533.2 eV corresponding to C–O–H is not shifted, which shows that this group does not interact with Pb(II) ions. The other two peaks moved slightly. The results indicated that the carboxylate groups and amide groups on the surface of EDBAMPS are involved in the adsorption process.[12] The N 1s spectrum of the EDBAMPS-Pb in Fig. 11d also showed a new peak, which indicates that the amino groups are also involved in the adsorption process.[37] All the results show that the coordination unit structure we designed successfully combines the mechanism of ion association and covalent coordination chelation.

4 Conclusions

In this work, a novel adsorbent with both anion group and neutral chelating group in the coordination unit was prepared by a preorganized structure strategy. Two carboxyl groups and four neutral coordination groups in the coordination unit interact with heavy metal ions simultaneously, showing a strong affinity of heavy metals. The prepared adsorbent has a maximum adsorption capacity of 352.1 mg g^{-1}. The

modification by amide group basically does not adsorb common interfering ions, such as K, Na, Ca, and Mg, and the presence of these ions indeed promotes the adsorption of heavy metal ions. This new adsorbent has good recycling performance and good application prospects.

Conflicts of interest

The author(s) declare that they have no conflict of interest.

Acknowledgements

This work was supported by the National Natural Science Foundation of China (No. 21876062), and the Natural Science Foundation of Shandong Province (No. ZR2017LB005).

Notes and references

1 Y. Huang, S. Zhang, Y. Chen, L. Wang, Z. Long, S. S. Hughes, S. Ni, X. Cheng, J. Wang, T. Li, R. Wang and C. Liu, *J. Hazard. Mater.*, 2020, **385**, 121528.
2 P. A. Turhanen, J. J. Vepsalainen and S. Peraniemi, *Sci. Rep.*, 2015, **5**, 1–8.
3 Y. Chang, J. Y. Lai and D. J. Lee, *Bioresour. Technol.*, 2016, **222**, 513–516.
4 F. Fu and Q. Wang, *J. Environ. Manage.*, 2011, **92**, 407–418.
5 M. Stasiak, M. Regel-Rosocka and A. Borowiak-Resterna, *Hydrometallurgy*, 2016, **162**, 57–62.
6 Z. A. Alothman and S. M. Wabaidur, *Arabian J. Chem.*, 2019, **12**, 633–651.
7 J. K. Mbadcam, S. G. Anagho, J. N. Nsami and A. M. Kammegne, *J. Environ. Chem. Ecotoxicol.*, 2011, **3**, 290–297.
8 T. Anitha, P. S. Kumar, K. S. Kumar, B. Ramkumar and S. Ramalingam, *Process Saf. Environ. Prot.*, 2015, **98**, 187–197.
9 H. Ravishankar, J. Wang, L. Shu and V. Jegatheesan, *Process Saf. Environ. Prot.*, 2016, **104**, 472–480.
10 I. Jilal, S. El Barkany, Z. Bahari, O. Sundman, A. El Idrissi, M. Abou-Salama, A. Romane, C. Zannagui and H. Amhamdi, *Carbohydr. Polym.*, 2018, **180**, 156–167.
11 A. Shahbazi, N. N. Marnani and Z. Salahshoor, *Biocatal. Agric. Biotechnol.*, 2019, **22**, 101398.
12 D. Lv, Y. Liu, J. Zhou, K. Yang, Z. Lou, S. A. Baig and X. Xu, *Appl. Surf. Sci.*, 2018, **428**, 648–658.
13 L. Li, X. Wang, M. Xie, H. Wang, X. Li and Y. Ren, *J. Membr. Sci.*, 2019, **578**, 95–102.
14 E. Repo, R. Koivula, R. Harjula and M. Sillanpää, *Desalination*, 2013, **321**, 93–102.
15 A. Mittal, M. Naushad, G. Sharma, Z. A. Alothman, S. M. Wabaidur and M. Alam, *Desalin. Water Treat.*, 2015, **57**, 21863–21869.
16 B. Li, F. Liu, J. Wang, C. Ling, L. Li, P. Hou, A. Li and Z. Bai, *Chem. Eng. J.*, 2012, **195–196**, 31–39.
17 Z. Zhang, X. Wang, H. Wang and J. Zhao, *Chem. Eng. J.*, 2018, **344**, 53–61.
18 L. F. Koong, K. F. Lam, J. Barford and G. McKay, *J. Colloid Interface Sci.*, 2013, **395**, 230–240.
19 Y. Markovska, M. Geneva, P. Petrov, M. Boychinova, I. Lazarova, I. Todorov and I. Stancheva, *Russ. J. Plant Physiol.*, 2013, **60**, 623–632.
20 M. S. Iorungwa, R. A. Wuana, S. G. Ylase and T. A. Tor-anyiin, *J. Environ. Earth Sci.*, 2014, **4**, 61–71.
21 J. Wang, Y. Li, Z. Lv, Y. Xie, J. Shu, A. Alsaedi, T. Hayat and C. Chen, *J. Colloid Interface Sci.*, 2019, **542**, 410–420.
22 Y. Liu, J. Xu, Z. Cao, R. Fu, C. Zhou, Z. Wang and X. Xu, *J. Colloid Interface Sci.*, 2020, **559**, 215–225.
23 J. Yu, S. Zhu, P. Chen, G.-T. Zhu, X. Jiang and S. Di, *Appl. Surf. Sci.*, 2019, **484**, 124–134.
24 X. Wan, M. A. Khan, F. Wang, M. Xia, W. Lei, S. Zhu, C. Fu and Y. Ding, *Chem. Eng. Res. Des.*, 2019, **152**, 95–105.
25 Y. Liu, Q. Gao, C. Li, S. Liu, K. Xia, B. Han and C. Zhou, *Chem. Eng. J.*, 2019, DOI: 10.1016/j.cej.2019.123610.
26 C. Jin, X. Zhang, J. Xin, G. Liu, J. Chen, G. Wu, T. Liu, J. Zhang and Z. Kong, *Ind. Eng. Chem. Res.*, 2018, **57**, 7872–7880.
27 Y. Song, N. Wang, L.-y. Yang, Y. g. Wang, D. Yu and X.-k. Ouyang, *Ind. Eng. Chem. Res.*, 2019, **58**, 6394–6401.
28 M. M. Abdallah, M. N. Ahmad, G. Walker, J. J. Leahy and W. Kwapinski, *Ind. Eng. Chem. Res.*, 2019, **58**, 7296–7307.
29 J. Chen, M. Yu, C. Wang, J. Feng and W. Yan, *Langmuir*, 2018, **34**, 10187–10196.
30 M. Musielak, A. Gagor, B. Zawisza, E. Talik and R. Sitko, *ACS Appl. Mater. Interfaces*, 2019, **11**, 28582–28590.
31 S. Tighadouini, S. Radi, M. Ferbinteanu and Y. Garcia, *ACS Omega*, 2019, **4**, 3954–3964.
32 Z.-j. Yi, J. Yao, H.-l. Chen, F. Wang, X. Liu and J.-s. Xu, *Desalin. Water Treat.*, 2015, **57**, 7245–7253.
33 X. Zhang, X. Wang and Z. Chen, *Materials*, 2017, **10**, 1–22.
34 X. Huang and M. Pan, *J. Mol. Liq.*, 2016, **215**, 410–416.
35 A. A. Taha, M. A. Shreadah, A. M. Ahmed and H. F. Heiba, *J. Environ. Chem. Eng.*, 2016, **4**, 1166–1180.
36 J. Ma, G. Zhou, L. Chu, Y. Liu, C. Liu, S. Luo and Y. Wei, *ACS Sustainable Chem. Eng.*, 2016, **5**, 843–851.
37 G. Li, J. Ye, Q. Fang and F. Liu, *Chem. Eng. J.*, 2019, **370**, 822–830.

